Original Paper

Evaluation of bubble removing performance in a TV glass furnace
Part 1. Mathematical formulation

Shinji Kawachi
Technology Department, Nippon Electric Glass Co. Ltd., Otsu, Shiga (Japan)

Yoshinori Kawase
Department of Applied Chemistry, Toyo University, Kawagoe, Saitama (Japan)

The bubble evolution and dissolution process in a glass furnace is an extremely complicated physico-chemical phenomenon. Most of the huge number of bubbles, generated in molten glass during the decomposition of the glass batch, are removed during the trajectory from the charging end to the forming section, but some remain in final products. On the basis of the two mechanisms, flotation and absorption, in the bubble removing process, a numerical simulator was developed to evaluate the influence of first, glass and batch composition, including refining agents, second, geometrical tank design and third, furnace operating conditions upon the bubble quality in products. In particular, the simulator enabled the estimation of the effect of refining gases which are caused by decomposition of the refining agents. Furthermore, an index was devised to synthetically assess the numbers of bubbles in final products. In part 1, the principles of the model which composes the simulator are described in mathematical formulation. The basic equations with boundary conditions and calculation procedures for thermal flow of molten glass, gas concentration in glass melt and gas evolvement from the refining agents are presented. The calculation strategy of the bubble removing process is also described.

Beurteilung der Effizienz der Blasenentfernung bei einem Schmelzofen für Fernsehröhrenglas
Teil 1. Mathematische Darstellung

Die Bildung und Auflösung von Blasen in einem Glasschmelzofen ist ein äußerst komplizierter physikalisch-chemischer Vorgang. Die meisten der sehr großen Menge an Blasen, die bei der Zersetzung des Glasgemenges im geschmolzenen Glas entstehen, werden im Laufe des Weges vom Einlegeende zum Formgebungsbereich entfernt. Ein Restbestand an Blasen gelangt jedoch ins Endprodukt. Unter Zugrundelegung der zwei Mechanismen bei der Blasenentfernung, nämlich der Flotation und Absorption, wurde ein numerischer Simulator entwickelt, um den Einfluß erstens, der Glas- und Gemengezusammensetzung, einschließlich der Läutermittel, zweitens, der Geometrie der Schmelzwanne und drittens, der Bedingungen des Ofenbetriebes auf die Art der Blasen in den Produkten zu bewerten. Insbesondere ermöglichte der Simulator die Einschätzung der Wirkung der Läutergase, die durch die Zersetzung der Läutermittel entstehen. Außerdem wurde ein Index entwickelt, um die Anzahl der Blasen im Endprodukt zu bestimmen. Im ersten Teil der Arbeit werden die Grundlagen des Modells, aus dem sich der Simulator zusammensetzt, mathematisch beschrieben. Die grundlegenden Gleichungen mit den Grenzbedingungen und Verfahren zur Berechnung des Wärmeflusses des geschmolzenen Glases, der Gaskonzentration in der Glasschmelze und der Gasentwicklung aus den Läutermitteln werden dargestellt. Ebenso wird die Vorgehensweise bei der Berechnung des Vorganges der Blasenentfernung beschrieben.

1. Introduction

The bubbles in glass products are commonly presumed to be created by the following processes. The glass batch charged into a furnace changes into glassy state by the heat of flame in the superstructure and/or by the Joule heat of electricity through the molten glass, which causes large amounts of gases to generate. The majority of gases generated by the decomposing reaction of the batch are released into the combustion chamber through the spaces of batch particles. However, some gases remain in the molten glass, become bubbles in the glass melt and are gradually carried to the forming area by the glass current in the furnace. Some bubbles veer off the flow line and escape through the glass surface. This phenomenon takes place because the bubble has buoyancy due to the difference in the density between the glass melt and the bubble gases. In addition, since gases in the bubble can diffuse into the glass melt, some bubbles may disappear as they travel in the furnace. In order to enhance such bubble removing function, refining agents are generally added to the glass batch. Glassware containing fewer bubbles have been manufactured by skillfully manipulating many variables based on long-term experience and keen intuition. Some bubbles can not be eliminated sufficiently by these degassing processes, and they stay in the product as glass defects.

In general, there are three factors which substantially influence the characteristics of bubbles in glass products. They are:

Received June 18, revised manuscript December 3, 1997.

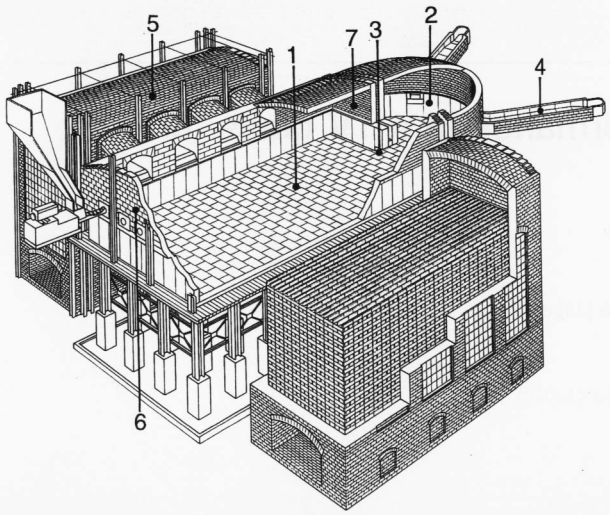

Figure 1. Schematic view of a TV glass furnace. 1: melter, 2: refiner, 3: throat, 4: feeder, 5: regenerator, 6: charging-end wall, 7: bridge wall.

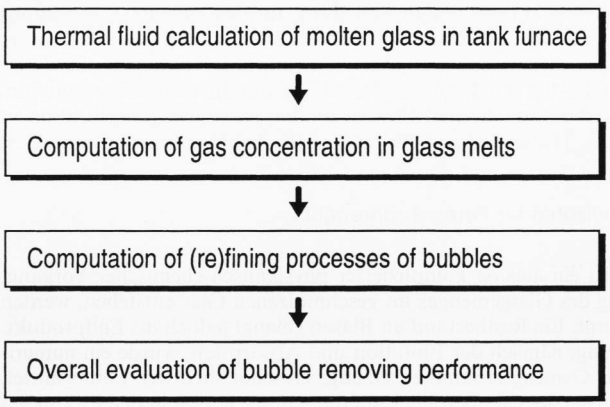

Figure 2. Submodels and computation procedure.

a) the glass and batch composition, including refining agents,

b) the geometrical design of the tank furnace, and

c) the operating conditions of the furnace.

It is one of glass engineers' dreams to be able to predict the bubble quality of the glass products when these process conditions are given.

Many research papers have been published with regard to the growth and the dissolution of bubbles, provided that the bubbles already exist in the molten glass [1 to 7]. However, not many models, in which all the above factors from a) through c) are taken into consideration and bubble quality can systematically be forecast, have been reported to date, although their need is strongly felt.

Schill et al. [8 and 9] disclosed that they made a simulator which connected the thermal fluid model of a three-dimensional furnace with a multicomponent bubble model. They stated that the simulator could trace the trajectory of a bubble and the change of the bubble size and composition. Unfortunately, only the simulated result was described and no details of their methodology was reported.

Ungan and Balkanli [10 to 15] pointed out the necessity for an overall simulation, by which glass flow and temperature distribution should be related to glass quality. They made the necessary formulations for modeling the (re)fining process. However, they did not take the effect of refining agents into consideration.

De Waal and Beerkens [16 and 17] mentioned an example of pursuing bubble behavior in the glass furnace. First of all, the temperature and flow pattern of the molten glass in the furnace were computed. In the next step, the concentration of dissolved gases in each part of the furnace was estimated. Furthermore, the trajectory of the bubbles, which had left the batch blanket and the refractory wall, was traced. By calculating the behavior of several thousands of bubbles, they concluded that it was possible to detect the difference of bubble removing performance with the change of furnace design and operating conditions. There was no explicit detail depicted concerning the movement and reaction of the refining agents in their papers.

In the above-mentioned papers, the possibility of predicting the bubble removing performance of the furnace was described. Only the simulated results of bubble behavior are reported, whereas no details were disclosed so that no one could replicate their results.

Kawachi et al. [18] published an overall model describing bubble behavior, which makes it possible to forecast the combustion air temperature preheated by regenerator, estimate the amount of the radiant heating onto the molten glass from flame and wall, compute the thermal convection and temperature distribution of the molten glass, and predict the bubble removing performance of the furnace. In their report, the thermal fluid analysis and the bubble removing behavior were calculated based on a two-dimensional model. In this paper, making some revisions, the authors have expanded the two-dimensional model to a three-dimensional one in order to reproduce the real furnace behavior in a more realistic manner. However, the regenerator model and the radiant heating model are omitted because they merely play a supplementary role in the bubble behavior model. This overall simulator which predicts the bubble removing performance of a furnace will be discussed.

2. Bubble removing model

2.1 Structure and calculating procedure of the model

The simulator which evaluates the bubble removing performance of a furnace (figure 1) is composed of the submodels explained in figure 2. Calculations are worked out according to the sequence as follows:

– Thermal fluid calculation of molten glass in tank furnace: The convection and temperature of the molten glass in the furnace are computed. Many research papers have been published in this field, so far [19 to 24].
– Computation of gas concentration in the melts: The concentration of the dissolved gases in the molten glass is procured. This model takes into consideration the following three major factors influencing the gas concentration in the melt:

a) refining gases (for instance, O_2, SO_2) generated from refining agents;

b) combustion gases in the superstructure (for instance, N_2, CO_2, O_2);
c) batch gases derived from initial reaction of the glass batch (for instance, N_2, CO_2, O_2, SO_2).

– Computation of (re)fining process of bubbles: Huge numbers of initial bubbles with various sizes are placed beneath the batch blanket and their trajectories are traced. The path of the bubbles is classified into four categories, as follows:

first, bubbles which disengage from the glass surface due to flotation;
second, bubbles which disappear in the molten glass due to absorption;
third, bubbles which flow out of feeder and might be detected in glass products;
fourth, bubbles which remain in the furnace after a given period of time.

– Overall evaluation of bubble removing performance: The number of bubbles raised to the glass surface and the number of bubbles absorbed into the glass melt are added. The process with the higher total number is judged to be superior in bubble removing performance.

2.2 Calculation of thermal flow of molten glass

2.2.1 Fundamental equations

In order to obtain the velocity and temperature distributions of the glass melt in a furnace, three governing equations, i.e. the continuity equation, the Navier-Stokes' motion equation and the energy equation are solved simultaneously. Each equation is described by the Cartesian tensor symbol.

On the assumption that glass is an incompressible fluid, the continuity equation is defined as:

$$\frac{\partial u_i}{\partial x_i} = 0 \,. \tag{1}$$

Applying the Boussinesq approximation to the unsteady Navier-Stokes' equation,

$$\frac{\partial u_i}{\partial t} + u_j \frac{\partial u_i}{\partial x_j} = -\frac{1}{\rho}\frac{\partial p}{\partial x_i} + \upsilon \frac{\partial^2 u_i}{\partial x_j^2} + K_i \tag{2}$$

is obtained, where $K_i = \{0, 0, g\beta(T - T_0)\}$.

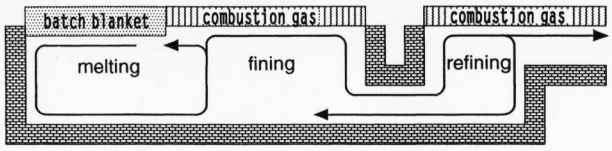

Figure 3. Conceptual function of a glass melting furnace.

The Rosseland approximation being applied, the unsteady energy equation may be written as:

$$\frac{\partial T}{\partial t} + u_i \frac{\partial T}{\partial x_i} = \lambda \frac{\partial^2 T}{\partial x_i^2} \,. \tag{3}$$

2.2.2 Numerical calculation method and boundary conditions

To solve the equations (1 to 3) numerically, the control volume method for discretization is adopted. The motion equation is calculated in the up-wind direction by the Successive Over-Relaxation (SOR) method [25]. In order to reduce the fluctuation of the solution, the staggered mesh technique is used, defining the velocity at the side of the calculation cell and defining the pressure and the temperature in the cell center [26]. In order to get the solution of the continuity equation, the Highly Simplified Marker And Cell (HSMAC) method is applied which releases velocity and pressure simultaneously [27].

As the boundary conditions, enforced inflow and outflow conditions are adopted at the inlet and the outlet of the molten glass. Namely, it is assumed that the fluid flows into the furnace at a uniform velocity from the batch blanket and the glass flows out at the exit of the refining chamber, i.e. the feeder entrance. The glass surface temperature including the batch area is given as the boundary condition of heat. The temperature distribution is decided according to data measured in the longitudinal direction in the superstructure of a real furnace. It is also supposed that there is no temperature gradient across the furnace. The heat flux boundary condition is employed in the refractory wall contacting the molten glass. This value is calculated in one direction through the wall, assuming the appropriate inside temperature of glass contact refractories and the cooling influence on them from outside.

2.3 Calculation of gas concentration in glass melt

2.3.1 Basic equations

The growth and shrinkage of a bubble are caused by diffusion, which is the result of the difference between the gas concentration in the bubble and in the melt. Accordingly, the gas concentration at each location of the molten glass in the furnace must be established in the next step. The three parameters mentioned in section 2.1 are considered to be the major factors that influence the gas concentration in the glass melt. The relationship among these factors is illustrated in figure 3.

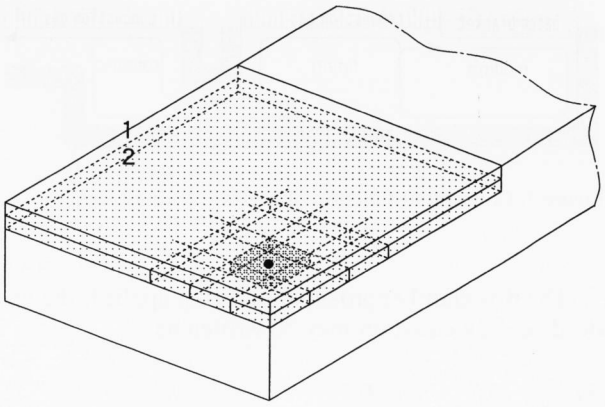

Figure 4. Schematic diagram of batch layer in melter. 1: batch layer, 2: glass melt contacting batch layer.

Taking the above factors into consideration, the unsteady diffusion equation concerning the gas concentration is solved to gain the concentration distribution of the gases in the molten glass in the velocity and temperature fields which have been determined by the thermal fluid analysis. The governing equation written in the Cartesian tensor expression is given as:

$$\frac{\partial C_k}{\partial t} + u_i \frac{\partial C_k}{\partial x_i} = D_k \frac{\partial^2 C_k}{\partial x_i^2} + \frac{S_k}{\Delta x \, \Delta y \, \Delta z} \tag{4}$$

where the subscript k denotes the sort of gases.

The molten glass surface is in contact with the batch blanket or the combustion gases. This interface becomes the boundary condition of equation (4). Moreover, the initial glass produced from the batch is presumed to pass through the furnace as shown by the arrow in figure 3. The refining agents are decomposed and the refining gas is evolved along the flow process. This phenomenon is described in the source term, the second term of the right-hand side of equation (4).

2.3.2 Gas evolved from refining agent

When batch changes into glass, a huge number of bubbles are created. If the gas concentration in the glass is higher than that in the bubble, the gases in the molten glass diffuse into the bubble, which increases the bubble diameter and promotes flotation. Refining agents such as antimony oxide, arsenic oxide and sodium sulfate, which generate O_2 and/or SO_2 gas in the molten glass, are added to the batch for this purpose. When the batch is charged into the furnace and is exposed to a high-temperature atmosphere, the refining agents tend to decompose and evolve the refining gas, which may dissolve into the glass melt. The gas generation is affected by the type of glasses, the batch composition and the temperature where the refining agents exist.

The chemical compound used as a refining agent is multivalent oxide. Antimony oxide is taken for instance. Antimony pentoxide exposed to high temperature releases oxygen gas to become antimony trioxide. This oxygen diffuses into the glass melt and promotes bubble removal. In contrast, antimony trioxide existing in high-temperature melts supposedly changes to pentoxide reversely as a result of its reaction with oxygen in the melt and bubbles. This phenomenon is also considered useful in absorbing the gases in bubbles, resulting in their deterioration. However, it was not clearly observed that such a reversible reaction occurred in the TV panel glass investigated here, which will be discussed in part 2. Therefore, only the decomposition reaction of the refining agents will be dealt with in this paper.

The gas generation rate from the refining agent S_k is defined as equation (5):

$$S_k = a_k \left(\frac{M_k}{Ms} \right) Ss \, . \tag{5}$$

For example, supposing the decomposition reaction of a refining agent, such as $Sb_2O_5 \rightarrow Sb_2O_3 + O_2 \uparrow$, one mole of Sb_2O_5 is known to produce one mole of Sb_2O_3, in which $a_k = 1$ where $M_k = 32$ g/mol and $Ms = 324$ g/mol. Ss is yielded by the reaction rate formula shown in equation (6):

$$Ss = \left(\frac{\mathrm{d}f}{\mathrm{d}t} \right) Q_0 = k f^n Q_0 \, . \tag{6}$$

Further, the reaction rate constant k is hypothesized to satisfy the Arrhenius' equation:

$$k = A \exp\left(- \frac{E}{R T} \right) . \tag{7}$$

The unknown parameters in equations (6 and 7), A, E and n, necessary for the analysis, can be determined by gas profile measurement. The data is obtained by heating the glass batch, including the refining agent, in a helium carrier gas and by measuring the evolved gas quantitatively.

Once all the unknown factors in equations (6 and 7) are calculated, the amount of evolving gas can be predicted on condition that the temperature and elapsed time are yielded.

2.3.3 Calculation of the amount of generated refining gas

Using the principle stated in section 2.3.2 the refining gas amount generated in the glass furnace can be computed according to the following procedure. Figure 4, which shows the batch charging end of the furnace from an elevated position, illustrates schematically where the batch blanket contacts the molten glass. Upper layer no. 1 shows the batch blanket and lower layer no. 2, lightly shadowed, denotes the molten glass in contact with the batch. It is hypothesized that initial glass is formed in layer no. 2, the refining agent begins to de-

compose and the evolution of refining gas starts there. Layer no. 2 is divided into small cells. A typical cell is shown in figure 4 as a darker shadowed cell. When the amount of the charged batch is divided by the number of all cells, the amount of the refining agent per cell can be determined. One particle, a "refining particle", shown by a filled circle in figure 4, is placed at the center of the cell. The gas generation capability of the refining agent in one cell is hypothesized to be concentrated on the refining particle.

The refining particle travels in part within various temperature fields along the glass flow in the furnace. The amount of the gas generated from the refining particle is calculated by applying equations (5 to 7) to each refining particle. During the time step Δt, if it is symbolized that the reacted amount of one refining particle is Ss_p, the amount of the gas generation owing to the reaction is Sp_k, and the generated gas concentration at each cell is Sc_k, they may have the following relationship expressed by equations (8 to 10):

$$Ss_p = k f^n Q_{p0} \Delta t \,, \tag{8}$$

$$Sp_k = a_k \left(\frac{M_k}{Ms} \right) Ss_p \,, \tag{9}$$

$$Sc_k = \Sigma \frac{Sp_k}{Ve} \,. \tag{10}$$

The location and the reacted amount of the refining particle are pursued until the remaining amount of the reacting potential becomes less than 0.01 % of its original amount or the particle leaves the system. The total amount of the refining gas at each cell is summed up. As a result of this calculation, the gas concentration at each cell can be acquired.

2.3.4 Boundary conditions

2.3.4.1 Boundary condition beneath batch blanket

The gas concentration in the melt beneath the batch blanket is presumed to be equal to the solubility governed by the glass composition and the temperature at its location. Gases in the glass, for instance, CO_2, N_2 and O_2, are sufficiently supplied by raw materials such as carbonate, nitrate and refining agents, and are influenced by combustion gases. Also, excessive gases over the solubility are presumed to become bubbles and to escape from the melt. Accordingly, the above assumption is thought to be a reasonable primary approximation.

Besides the methodology stated above, the following approaches will be possible for estimating the gas amount dissolved at the batch/glass melt boundary:

a) sampling the initial glass from a real furnace and measuring the dissolved gases directly,

b) melting batch in a crucible according to the same thermal history as the batch melting in the real furnace and measuring the dissolved gases in the melt,

c) devising a mathematical model of the gas evolution in melting the batch [10].

The approach used in this work will be described in section 3.3.2.

2.3.4.2 Boundary conditions in contact with combustion gases

The gas composition over the glass melt is obtained by analyzing the combustion gases in a real furnace or by using a combustion model. The gas concentration in the molten glass at the boundary is calculated from the partial pressure of the combustion gas, whose governing model is described by Henry's law as equation (11):

$$C_k = L_k N_k \,. \tag{11}$$

In a side-port furnace, it is empirically known that the highest temperature should be attained near the center of the longitudinal direction through the melter and a slightly lower temperature should be kept at the charging end and the bridge wall of the furnace in order to melt better-quality glass. For the purpose of achieving such a temperature profile, the amount of fuel consumption and combustion air at each port are adjusted. In addition, excessive air is often fed into the refiner because the main function of the refiner is to cool the molten glass, so that it will achieve a suitable temperature for the forming process. Accordingly, the combustion gas composition at each cell on the glass surface is different.

2.4 Calculation of bubble removing process

2.4.1 Outline

The principles necessary for describing the process of bubble dissolution or the removal of a bubble from the furnace as a defect in a product are discussed here. In this simulation the bubbles are regarded as being created at the batch/glass melt boundary as the batch is converted to glassy state. These bubbles move along the convection currents of the molten glass in the furnace. During this process the gases are transferred by the concentration difference between the gases in the bubble and those in the melt. This gas exchange and the temperature environment change along the bubble movement cause a change in the diameter and buoyancy of the bubble. In the bubble moving process, by both convection and flotation, bubbles primarily disappear by escaping from the glass surface or by being dissolved into the glass melt. However, the bubbles which do not escape or dissolve and are larger than the product specification may become the cause of product rejects.

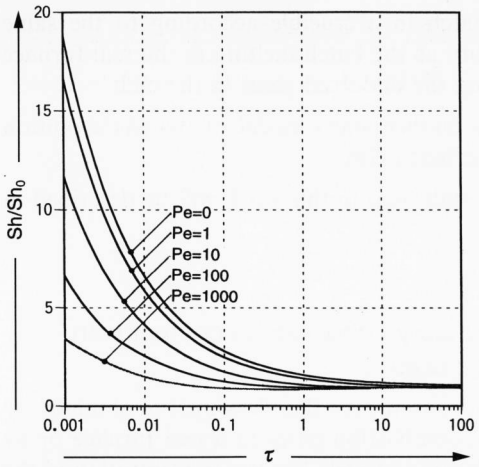

Figure 5. Relationship of τ and Sh/Sh_0 at various Pe numbers (equations (14 to 17)).

2.4.2 Basic equations regarding the bubble removing process

2.4.2.1 Ascending velocity of a bubble

The ascending velocity of a bubble in glass melt Vs is hypothesized to follow Stokes' law [28] as given in equation (12):

$$Vs = \frac{2}{9} \frac{g r^2 \rho}{\eta} . \tag{12}$$

2.4.2.2 Gas exchange between a bubble and glass melt

The difference between the gas concentration in the glass at the bubble/glass melt boundary Ca_k and the gas concentration in the glass bulk Cb_k becomes the driving force which makes the gas transfer from the higher concentration side to the lower one. Since the surface area of a bubble is given as $4\pi r^2$, the weight of the inflow gas through the bubble surface per unit of time I_k may be described as follows:

$$I_k = 4\pi r^2 k_{Lk} (Cb_k - Ca_k) . \tag{13}$$

The Sherwood number at unsteady state Sh is given as:

$$\begin{aligned} Sh_k &= \frac{k_L (2r)}{D_k} \\ &= 2\left(1 + \frac{1}{\sqrt{\pi \tau_k}}\right) + B_k \cdot Pe_k^{1/3} \cdot \\ &\quad \cdot \left[0.956 + \left(\frac{2}{\sqrt{\pi \tau_k}} Pe_k^{1/3}\right)^5\right]^{1/5} . \end{aligned} \tag{14}$$

The mass transfer coefficient k_L, if $Pe_k > 1000$, can be regarded as the value at $Pe_k = 1000$.

Moreover, the interpolation coefficient B_k in equation (14) is obtained by the result shown in the graph of Abramzon's paper [29].

$$\begin{aligned} B_k = &- 0.166 + 0.177\, y - 0.00751\, y^2 - \\ &- 0.00669\, y^3 - 0.00242\, y^4 + \\ &+ 0.260\, z + 0.08270\, z^2 - 0.02770\, z^3 \end{aligned} \tag{15}$$

where

$$y = \ln(\tau_k)/\ln(10) \tag{16}$$

and

$$z = \ln(Pe_k)/\ln(10) . \tag{17}$$

When B_k evaluated by equation (15) is less than 0, it is regarded as $B_k = 0$.

For $0 \leqq Pe \leqq 1000$, there exists the relationship shown in figure 5 between τ and Sh/Sh_0, provided that the Sherwood number at steady state is Sh_0.

2.4.2.3 Equation of state for gas

The gas in a bubble is assumed to change according to the law of ideal gas shown in equation (18):

$$P_k V = \frac{m_k}{M_k} R T . \tag{18}$$

The total pressure against a bubble being expressed as P becomes $P = \Sigma P_k$.

2.4.2.4 Gas concentration at the gas/glass melt boundary

At the place where gas contacts liquid, the gas concentration in the liquid at the boundary is assumed to follow Henry's law [1], given in equation (11). This law describes the situations in which the combustion gas contacts the molten glass and the gas in the bubble touches the glass melt.

2.4.3 Change of diameter and composition of a bubble by gas exchange

When a small time step is assumed to be Δt, Δt_n is regarded as the time which a bubble takes to reach any cell side or the time until $t + \Delta t$ elapses. With the assumption that m_k is the gas weight in a bubble at the starting time of computation and m_k^* is the gas weight after Δt_n has lapsed, the change of gas weight m_k^* is expressed by the following equation (19):

$$m_k^* = m_k + I_k \Delta t_n . \tag{19}$$

At the same time, the volume V and the radius r of the bubble will change in accordance with equations (20 and 21):

$$V = \sum \frac{m_k^*}{M_k} \frac{RT}{P_k}, \tag{20}$$

$$r = \left(\frac{3V}{4\pi}\right)^{1/3}. \tag{21}$$

Gas pressure P of a bubble in glass melt is expressed by equation (22):

$$P = P_0 + \rho g h + 2\sigma/r. \tag{22}$$

The volume change described in equation (20) causes the pressure change in the bubble, which will follow equation (18).

Finally, the partial pressure ratio of gas element k in the bubble N_k may be calculated according to equation (23):

$$N_k = P_k/P. \tag{23}$$

2.4.4 Computation procedure of the bubble removing process

Using the basic equations stated in sections 2.4.2 and 2.4.3, the trajectories of all the bubbles generated beneath the batch blanket can be pursued. Figure 6 shows the calculation flow of the procedure, which accounts for the details in the following:

a) Starting the calculation.

b) Setting the starting condition of a bubble.
A bubble with a given gas composition N_k of radius r is assumed to be created at a cell.

c) Calculating the volume and weight of the bubble.
The volume of the bubble is calculated as $V = 4\pi r^3/3$. The gas weight in the bubble is obtained by the transformation of equation (18), where T is the cell temperature.

d) Deciding the time step for loop calculation.
The bubble movement is calculated at every short time step Δt. The value of Δt should be given beforehand as input data. The elapse time is accumulated as $t = t + \Delta t$ by the loop calculation.

e) Identifying the cell number where the bubble exists.

f) Referring to the glass velocity in the cell and adding the ascending velocity.

Because molten glass velocity is defined at the cell side, the speed and direction of the bubble are calculated based on the weighted average of those values. The bubble ascending velocity is obtained according to equation (12), from the assumed bubble diameter. This value is superimposed onto the glass flow velocity.

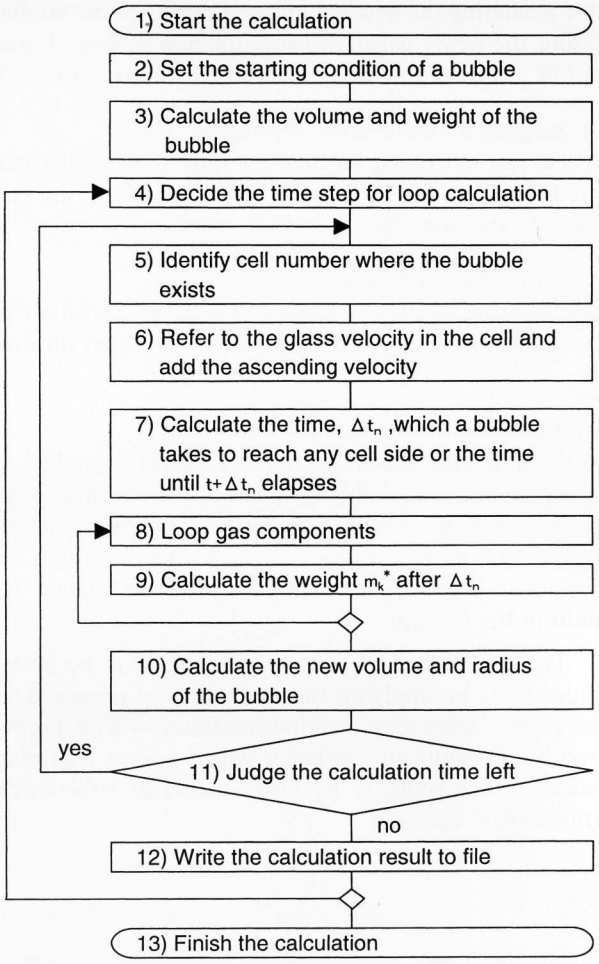

Figure 6. Flow chart of calculation of bubble trajectory.

g) Calculating the time Δt_n.
Δt_n is the time which a bubble takes to reach any cell side or the time until $t + \Delta t$ elapses. During the set time step Δt, there are three possibilities regarding its location. These are: first, the bubble moves into the neighboring cell, second, the bubble reaches the cell boundary, or third, the bubble continues to exist inside the cell. In the first case, the required time for the bubble to reach the cell boundary from the original position must be calculated again.

h) Calculating each gas element sequentially by means of a calculation loop.

i) Calculating the weight m_k^* after Δt_n.
The weight of each gas element m_k^* after Δt_n is given by equation (19). The gas weight I_k, which flows in or out of the bubble, is yielded by equation (13). Gas concentration at the bubble/glass melt boundary Ca_k used in equation (13) is decided by equation (11). Furthermore, the partial gas pressure N_k in equation (11) is given by equations (18 and 23). The above-mentioned calculations are repeated on all the gas elements.

j) Calculating the new volume and radius of the bubble. Using the newly calculated m_k^*, the new volume V and radius r can be obtained based on equations (20 to 22).

k) Judging the calculation time left.
When the scheduled calculation time is over, the calculation is ended. But if it is within the time, the calculation is continued.

l) Writing the calculation result to file.
The location, the diameter and the gas composition of the bubble at each calculation loop are written on disk file.

m) Finishing the calculation.
In the next step, the trajectory calculation is applied to a large number of bubbles. It is possible to investigate the whereabouts of the bubbles, whether they are removed by flotation or absorption, they pass through the furnace to become defects in glass products, or they remain in the furnace.

The mechanism of removing bubbles will be better understood by applying the methodology proposed in this paper. Better glass-making conditions will be discovered by changing the variables which govern (re)fining processes, occasionally by more than can be inferred from a real furnace.

3. Nomenclature

3.1 Symbols

a	mole ratio of system of product and system of reactant
A	frequency factor in s^{-1}
B	interpolation coefficient
C	gas concentration in kg/m^3
Ca	gas concentration at bubble/glass melt boundary in kg/m^3
Cb	gas concentration in glass melt in kg/m^3
D	gas diffusivity in m^2/s
E	activation energy in J/mol
f	ratio of unreacted amount against total amount of refining agent
g	gravitational acceleration in m/s^2
h	distance between a bubble and glass melt surface in m
I	gas amount transferring into/out of a bubble in kg/s
k	reaction rate constant in s^{-1}
k_L	mass transfer coefficient in m/s
K	force to unit mass in m/s^2
L	gas solubility in kg/m^3
m	gas weight in a bubble in kg
m^*	gas weight in a bubble after Δt_n time in kg
M	molecular weight of generated gas or gas in a bubble
Ms	molecular weight of refining agent
n	reaction order
N	partial gas pressure in Pa
p	pressure in glass melt in Pa
P	gas pressure in a bubble in Pa
P_0	atmospheric pressure in Pa
Pe	Péclet number $Pe = (2 r V_s)/D$
Q_0	reaction potential at initial stage in kg, i.e. value of charging rate of refining agent divided by reaction rate constant
Q_{p0}	gas generation potential of a refining particle in kg
r	bubble radius in mm
R	gas constant in J/(mol K)
S	gas generation rate from refining agent in kg/s
Sc	gas concentration evolved in a cell in kg/m^3
Sh	Sherwood number at an unsteady state
Sh_0	Sherwood number at a steady state $Sh_0 = 1 + (1 + Pe)^{1/3}$
Sp	generated gas amount of a refining particle in kg
Ss	reacted amount of refining agent in kg
Ss_p	reacted amount of a refining particle in kg
t	time in s
Δt	time step in s
Δt_n	time which a bubble takes to reach any cell side or the time $t + \Delta t$ elapses in s
T	temperature in K
T_0	reference temperature in K
u	velocity in m/s
V	bubble volume in m^3
Ve	cell volume in m^3
Vs	bubble rising velocity in m/s
x	length in m
Δx, Δy, Δz	lengths of unit cell in m
β	volume expansion coefficient in K^{-1}
η	viscosity in Pa s
λ	thermal conductivity in W/(m K)
ν	kinematic viscosity in m^2/s
ρ	density in kg/m^3
σ	surface tension in N/m
τ	dimensionless time $\tau = (Dt)/r^2$

3.2 Subscripts

i	direction
j	direction
k	sort of gases

4. References

[1] Krämer, F.: Mathematisches Modell der Veränderung von Gasblasen in Glasschmelzen. Glastech. Ber. **52** (1979) no. 2, p. 43–50.

[2] Weinberg, M. C.; Onorato, P. I. K.; Uhlmann, D. R.: Behavior of bubbles in glassmelts. Pt. 1. Dissolution of a stationary bubble containing a single gas. J. Am. Ceram. Soc. **63** (1980) no. 3–4, p. 175–180.

[3] Weinberg, M. C.; Onorato, P. I. K; Uhlmann, D. R.: Behavior of bubbles in glassmelts. Pt. 2. Dissolution of a stationary bubble containing a diffusing and a nondiffusing gas. J. Am. Ceram. **63** (1980) no. 7–8, p. 435–438.

[4] Onorato, P. I. K.; Weinberg, M. C.; Uhlmann, D. R.: Behavior of bubbles in glassmelts. Pt. 3. Dissolution and growth of a rising bubble containing a single gas. J. Am. Ceram. Soc. **64** (1981) no. 11, p. 676–682.

[5] Němec, L.: The behaviour of bubbles in glass melts. Pt. 1. Bubble size controlled by diffusion. Glass Technol. **21** (1980) no. 3, p. 134–138.

[6] Němec, L.: The behaviour of bubbles in glass melts. Pt. 2. Bubble size controlled by diffusion and chemical reaction. Glass Technol. **21** (1980) no. 3, p. 139–144.

[7] Cable, M.; Frade, J. R.: Theoretical analysis of the dissolution of multi-component gas bubbles. Glastech. Ber. **60** (1987) no. 11, p. 355–362.

[8] Schill, P.; Chmelař, J.: Bubbles behaviour in the glass melting tank. In: 2nd International Conference "Advances in the Fusion and Processing of Glass", Düsseldorf 1990. Poster Abstracts. Frankfurt/M.: Deutsche Glastech. Ges., 1990. p. 45–49.

[9] Chmelař, J.; Franek, A.; Schill, P.: Computer aided tracing of bubbles – glass quality control. In: XVI International Congress on Glass, Madrid 1992. Proc. Vol. 6. p. 45–50. (Bol. Soc. Esp. Ceram. Vid. 31-C (1992) 6.)
[10] Ungan, A.: Three dimensional numerical modeling of glass melting process. Purdue Univ., West Lafayette, IN (USA), Ph. D. thesis 1985.
[11] Ungan, A.: Three dimensional numerical simulation of fining process in glass melting furnaces: mathematical formulation. In: 2nd International Conference "Advances in the Fusion and Processing of Glass", Düsseldorf 1990. Glastech. Ber. **63K** (1990) p. 19–28.
[12] Balkanli, B.; Ungan, A.: Numerical simulation of bubble behaviour in glass melting tanks. Pt. 1. Under ideal conditions. Glass Technol. **37** (1996) no. 1, p. 29–34.
[13] Balkanli, B.; Ungan, A.: Numerical simulation of bubble behaviour in glass melting tanks. Pt. 2. Dissolved gas concentration. Glass Technol. **37** (1996) no. 3, p. 101–105.
[14] Balkanli, B.; Ungan, A.: Numerical simulation of bubble behaviour in glass melting tanks. Pt. 3. Bubble trajectories. Glass Technol. **37** (1996) no. 4, p. 137–142.
[15] Balkanli, B.; Ungan, A.: Numerical simulation of bubble behaviour in glass melting tanks. Pt. 4. Bubble number density distribution. Glass Technol. **37** (1996) no. 5, p. 164–168.
[16] Waal, H. de: Mathematical modeling of the glass melting process. In: 2nd International Conference "Advances in the Fusion and Processing of Glass", Düsseldorf 1990. Glastech. Ber. **63K** (1990) p. 1–18.
[17] Beerkens, R. G. C.: The role of gases in glass melting processes. Glastech. Ber. Glass Sci. Technol. **68** (1995) no. 12, p. 369–380.
[18] Kawachi, S.; Nagao, H.: Method for evaluating bubble refining performance in a continuous glass melting furnace. Jap. pat. no. 197327. Date of filing: Dec. 26, 1989, date of publ.: Aug. 28, 1991.
[19] Clomburg, L.: Mathematical and experimental modeling of the circulation patterns in glass melts. Massachusetts Institute of Technology, Cambridge, MA (USA), Ph. D. thesis 1971.
[20] Mase, H.; Sasagawa, Y.: Mathematical modeling of glass tank furnace. Rep. Res. Lab. Asahi Glass Co. **23** (1973) no. 2, p. 101–127.
[21] Mase, H.; Oda, K.: Mathematical model of glass tank furnace with batch melting process. J. Non-Cryst. Solids **38 & 39** (1980) p. 807–812.
[22] Ungan, A.; Viskanta, R.: Three-dimensional numerical modeling of circulation and heat transfer in a glass melting tank. Pt. 1. Mathematical formulation. Glastech. Ber. **60** (1987) no. 3, p. 71–78.
[23] Ungan, A.; Viskanta, R.: Three-dimensional numerical modeling of circulation and heat transfer in a glass melting tank. Pt. 2. Sample simulations. Glastech. Ber. **60** (1987) no. 4, p. 115–124.
[24] Mase, H.; Iga, M.; Itoh, H. et al.: Glass furnace simulator and the recent trend. Glass (Japan) (1995) no. 38, p. 24–31.
[25] Smith, G. D.: Numerical solution of partial differential equations. Oxford: Oxford Univ. Press, 1985. p. 230–234.
[26] Patankar, S. V.: Numerical heat transfer and fluid flow. New York: Hemisphere Publ. Corp., 1980. p. 118–123.
[27] Arakawa, C.: Computational fluid dynamics for engineering. Tokyo: Univ. of Tokyo Press, 1994. p. 157–158.
[28] Jebsen-Marwedel, H.; Brückner, R.: Glastechnische Fabrikationsfehler. 3. Aufl. Berlin (et al.): Springer, 1980. p. 222–224.
[29] Abramzon, B. M.; Rivkind, V. Y.; Fishbein, G. A.: Unsteady mass transfer with a heterogeneous chemical reaction during laminar flow past a sphere. Inz.-Fiz. Zh. **30** (1976) no. 1, p. 73–79.

0498P001

Addresses of the authors:

S. Kawachi
Nippon Electric Glass Co., Ltd.
Technology Department
7-1, Seiran, 2-Chome
Otsu, Shiga 520 (Japan)

Y. Kawase
Toyo University
Department of Applied Chemistry
Faculty of Engineering
Kujirai, Kawagoe-Shi, Saitama 350 (Japan)